Check for updates

*Original Research Article*

# Effect of Qibai Pingfei Capsules on the HMGB1/TLR4/NF-κB Signaling Axis in CSE-induced Inflammation of 16HBE Cells

Pharmacognosy Magazine
22(3) 831–841, 2026
© The Author(s) 2025
Article reuse guidelines:
in.sagepub.com/journals-permissions-india
DOI: 10.1177/09731296251364981
journals.sagepub.com/home/phm



**Li Fang[1], Lu Zhang[2], Mengyao Shi[2], Cheng Yang[1], Jiabing Tong[2], Yating Gao[1] and Zegeng Li[1,2,3]**

## Abstract

**Background and Objectives:** Chronic inflammation resulting from cigarette smoke extract (CSE) is frequently driven by activation of the high mobility group box 1 (HMGB1)–toll-like receptor 4 (TLR4)–nuclear factor kappa B (NF-κB) signaling cascade. This study was designed to explore the regulatory influence of Qibai Pingfei Capsules (QBPF) on inflammation-related pathways in 16HBE cells, a human bronchial epithelial cell line, following CSE treatment. We also assessed the impact of QBPF on NF-κB signaling dynamics and cytokine production using a co-culture model with THP-1-derived macrophages.
**Materials and Methods:** Levels of inflammatory mediators were quantified via enzyme-linked immunosorbent assay and quantitative reverse transcription polymerase chain reaction, while protein expression and intracellular localization were analyzed through Western blotting and immunofluorescence. NF-κB activity was further verified by RNA interference and overexpression techniques.
**Results:** QBPF markedly mitigated the inflammatory responses induced by CSE, as evidenced by decreased cytokine output and reduced transcription of HMGB1, toll-like receptor 2, TLR4, and myeloid differentiation primary response gene 88. Furthermore, QBPF hindered the nuclear translocation of NF-κB and disrupted upstream molecular events linked to its activation.
**Conclusion:** QBPF demonstrates potent anti-inflammatory potential through modulation of NF-κB-associated signaling networks. The current findings emphasize QBPF's value as a prospective therapeutic candidate for controlling smoke-induced airway inflammation and suggest its broader applicability to respiratory disorders characterized by chronic inflammation.

## Keywords

Qibai Pingfei Capsules, chronic obstructive pulmonary disease, HMGB1/TLR4/NF-κB pathway, cigarette smoke extract, inflammation

**Received** 29 April 2025; **revised** 29 May 2025; **accepted** 03 July 2025

## Introduction

Tobacco use remains a significant global health concern, being strongly correlated with a broad range of respiratory ailments, including chronic bronchitis, pulmonary cancers, and chronic obstructive pulmonary disease (COPD) (Christenson et al., 2022; Leiter et al., 2023). The pathological effects of tobacco smoke are largely attributed to its potent inflammatory potential, especially in the bronchial airways. Exposure to cigarette smoke extract (CSE), which comprises a complex mixture of harmful chemicals, provokes intense inflammatory reactions in bronchial epithelial cells (Kosmider et al., 2011; Yoshida et al., 2019). These persistent inflammatory insults are considered key contributors to the onset and progression of smoking-associated respiratory diseases (Elisia et al., 2020; Kotlyarov, 2023).

[1]Department of Respiratory Medicine, First Affiliated Hospital of Anhui University of Traditional Chinese Medicine, Hefei, Anhui, China
[2]Graduate School, Anhui University of Chinese Medicine, Hefei, Anhui, China
[3]Anhui Provincial Key Laboratory, Anhui University of Chinese Medicine, Hefei, Anhui, China

**Corresponding author:**
Zegeng Li, Department of Respiratory Medicine, First Affiliated Hospital of Anhui University of Traditional Chinese Medicine, Hefei, Anhui 230001, China.
E-mail: fangli0825@163.com

Creative Commons Non Commercial CC BY-NC: This article is distributed under the terms of the Creative Commons Attribution-NonCommercial 4.0 License (http://www.creativecommons.org/licenses/by-nc/4.0/) which permits non-Commercial use, reproduction and distribution of the work without further permission provided the original work is attributed as specified on the SAGE and Open Access pages (https://us.sagepub.com/en-us/nam/open-access-at-sage).

CSE acts as a potent initiator of inflammation, triggering a cascade involving various intracellular signaling routes, among which the high mobility group box 1 (HMGB1)–toll-like receptor 4 (TLR4)–nuclear factor kappa B (NF-κB) axis is notably pivotal (Ying et al., 2021; Wang et al., 2020). When epithelial cells experience noxious stimulation or damage, they actively release HMGB1, a well-known damage-associated molecular pattern (DAMP). Once released, HMGB1 interacts with TLR4 present on immune cells, consequently triggering the downstream NF-κB signaling pathway (Chen et al., 2022; Idoudi et al., 2023). Acting as a principal transcriptional regulator, NF-κB governs the expression of multiple pro-inflammatory mediators that drive chronic inflammation (Liu et al., 2017; Yu et al., 2020). Extensive experimental evidence has demonstrated that CSE exposure increases the levels of HMGB1, TLR4, and NF-κB, thereby reinforcing the relevance of this signaling network as a potential intervention point in tobacco-related airway inflammation (Le et al., 2020; Wang et al., 2019).

Traditional Chinese Medicine (TCM) has been employed for centuries to address respiratory conditions. Among the various herbal formulations, Qibai Pingfei Capsules (QBPF) have garnered attention for their anti-inflammatory properties (Jia et al., 2022; Zhu et al., 2018). Accumulating evidence suggests that QBPF enhances lung function and mitigates inflammation in COPD-like models by influencing immune homeostasis—particularly the Th17/Treg balance—and modulating the gut–lung microbiome (Leiter et al., 2023). Additional investigations have indicated that QBPF may exert its pharmacological effects through modulation of intracellular signaling cascades such as the PI3K/AKT and mitochondrial pathways, which may trigger apoptosis in pulmonary arterial smooth muscle cells subjected to hypoxic stress (Christenson et al., 2022). Nonetheless, how QBPF affects the HMGB1–TLR4–NF-κB axis during CSE-related airway inflammation remains incompletely understood. This study investigates the regulatory involvement of QBPF in CSE-stimulated 16HBE bronchial epithelial cells, aiming to clarify its role within the associated signaling pathway. By clarifying the molecular mechanisms underpinning its anti-inflammatory potential, we aim to lay the groundwork for developing novel therapeutic approaches targeting smoke-related respiratory conditions. These insights may help inform future interventions aimed at managing chronic pulmonary inflammation.

## Materials and Methods

### *Drugs and Reagents*

QBPF (composition: *Astragalus*, raw ginseng, Chuanxiong, *Allium macrostemon*, Tinglizi, *Schisandra*, earthworm) were provided by the Preparation Center of the First Affiliated Hospital of Anhui University of Chinese Medicine (specification: 400 mg/capsule, batch no.: 20230106); PDTC (catalog no.: S30342, Shanghai Yuanye Bio-Technology Co. Ltd., Shanghai, China); lipopolysaccharide (catalog no.: L2689, Sigma, St. Louis, MO, USA); enzyme-linked immunosorbent assay (ELISA) detection kits: NF-κB, interleukin-6 (IL-6), tumor necrosis factor-alpha (TNF-α) (batch no.: JYM0028Ra, JYM0419Ra, JYM0635Ra, Wuhan GeneMean Bio-Technology Co. Ltd., Wuhan, China); goat anti-mouse IgG, goat anti-rabbit IgG (batch nos.: 140193, 202700514, Zsbio, Oberkochen, Germany); HMGB1, toll-like receptor 2 (TLR2), NF-κB antibodies (batch no.: 10017763, Bioss, Woburn, MA, USA).

### *Differentiation of THP-1 Monocytes into Macrophages*

THP-1 monocytic cells were maintained in Roswell Park Memorial Institute-1640 (RPMI-1640) medium, supplemented with 10% heat-inactivated fetal bovine serum (FBS) and 1% penicillin–streptomycin solution. Cultures were kept at 37°C under a humidified atmosphere containing 5% $CO_2$. To induce differentiation into macrophage-like phenotypes, cells were seeded and exposed to 80 ng/mL phorbol 12-myristate 13-acetate (PMA; Sigma–Aldrich) for a duration of 24 h. Following stimulation, PMA was removed by washing the cells twice using phosphate-buffered saline (PBS). Subsequently, cells were transferred to PMA-free RPMI-1640 medium and incubated for an additional 24 h to allow stabilization of macrophage characteristics. This differentiation protocol was optimized to enhance the expression of macrophage-specific surface molecules such as CD14, confirming successful conversion.

### *Preparation of CSE*

A self-made gas extraction device was used. Specifically, the device consisted of a combustion chamber connected via a rubber tube to a sterile glass bottle containing 15 mL of Dulbecco's Modified Eagle Medium (DMEM) high-glucose medium. The opposite end of the setup included a peristaltic pump that controlled the airflow to ensure consistent smoke delivery. One cigarette (Xiongshi brand, with 8 mg tar, 0.7 mg nicotine, and 10 mg CO per cigarette) was lit and inserted into the combustion chamber. Smoke was actively drawn through the tubing using negative pressure generated by the pump. Smoke was bubbled through the medium until the cigarette burned down to 5 mm from the filter, at which point the system was turned off. The culture bottle was gently shaken until no smoke bubbles were visible. The absorbance at 320 nm (A320) was determined using a spectrophotometer, and when it reached 1.0 ± 0.05, the solution was recognized as 100% CSE (Facchinetti et al., 2007). The extract was immediately passed through a 0.22 μm sterile membrane to remove particulates, then stored at –80°C and diluted as needed for subsequent experiments.

### Screening of Co-culture Concentrations for Macrophages and 16HBE Cells with the Cell Counting Kit-8 (CCK8)

THP-1 monocytes were cultured and plated in 12-well plates and differentiated into macrophages by adding 162 nM PMA on day 0. Subsequently, 16HBE cells were digested, and after stopping the digestion, the cells were centrifuged, and the culture medium was discarded. Cells were then plated into 96-well plates according to the cell numbers listed in Table 1. Macrophage MC cells were also plated into Transwell chambers according to the cell numbers listed in Table 1. The co-culture was established in a Transwell system, with macrophages placed in the upper inserts and 16HBE cells seeded into the lower wells. Each ratio was tested in triplicate. After 0, 24, 48, and 72 h of culture, the chambers were removed, and the CCK8 was applied to detect cell viability.

### Screening of Optimal Concentration and Time for the Combined Action of CSE, Hypoxia, and QBPF

A total of 10 independent migration assays were performed by placing macrophages into the upper chamber of a 24-well Transwell system. After cell adhesion and proliferation, CSE was prepared at four gradient concentrations (2%, 4%, 8%, and 16%), alongside a blank control, and introduced into the co-culture system. The plates were then transferred either to a normoxic incubator (20% $O_2$, 5% $CO_2$, 75% $N_2$) or to a tri-gas chamber mimicking hypoxic conditions (3% $O_2$, 5% $CO_2$, 92% $N_2$), and incubated for one of four predetermined durations: 6, 12, 24, or 48 h, to simulate *in vitro* features of COPD. To replicate the hypoxic microenvironment of inflamed bronchial tissue in COPD, the tri-gas incubator was used, with 3% $O_2$ selected based on prior evidence demonstrating optimal inflammatory activation. The proliferation of 16HBE cells under various CSE concentrations and oxygen conditions was assessed via the CCK8 assay to determine the most suitable exposure protocol. Lyophilized CSE powder was reconstituted into five different doses (0, 5, 10, 20, 60, and 80 μg/mL) and applied to the culture setup. These treatments were again subjected to the same four exposure durations to evaluate the inflammatory response dynamics.

### NF-κB Gene Silencing and Overexpression Experiment

Log-phase 16HBE cells were enzymatically dissociated, pelleted by centrifugation, and resuspended uniformly. Cells were then allocated into plates at a final concentration of $2.0 \times 10^5$ cells/mL. For downstream transfection, four RNase-free 1.5 mL microcentrifuge tubes were prepared, each containing 125 μL of serum and antibiotic free high glucose DMEM, pre-warmed to 37°C. Two of the tubes were treated with siRNA specifically targeting NF-κB or its negative control, while the remaining tubes received equivalent volumes of PCDNA3.0-based plasmid vectors. After thorough mixing by gentle pipetting to ensure even distribution, 4 μL of Lipo8000 transfection reagent was introduced into each sample. Following an incubation period ranging from 24 to 48 h, transfection outcomes were evaluated using quantitative reverse transcription polymerase chain reaction (qRT-PCR). All experiments were independently repeated three times ($n = 3$) to ensure reproducibility and reliability of the results.

### Detection of NF-κB Pathway-related Gene Expression by qRT-PCR

16HBE cells were enzymatically detached, pelleted, and resuspended in full growth medium, then distributed into six-well culture plates at a concentration of $2.0 \times 10^5$ cells/mL, using 2 mL per well. After incubation, total RNA was extracted from the harvested cells. Reaction mixtures for qPCR were assembled in nuclease-free Eppendorf tubes using the SYBR SuperMix Plus kit (Novostart), according to the manufacturer's protocol. All experiments were independently executed and repeated a minimum of three times ($n = 3$).

### Western Blot Detects the Related Protein Expression

The proteins were extracted from cells and denatured after adding protein lysis buffer. Following a blocking period of 1 h. The membranes were co-cultured with primary antibodies for 24 h. Subsequently, the membranes were washed with Tris-buffered saline with Tween (TBST) for a period of

**Table 1.** The Primer Sequences.

| Gene | Amplicon Size (bp) | Forward Primer (5′–3′) | Reverse Primer (5′–3′) |
|---|---|---|---|
| *β-actin* | 96 | CCCTGGAGAAGAGCTACGAG | GGAAGGAAGGCTGGAAGAGT |
| *HMGB1* | 115 | ATACATCTCAGGGCCAAACC | AACTTTGCTCCAAAGAGGGA |
| *TLR2* | 93 | TTCTCCCAGTGTTTGGTGTT | CTGTCTTCCTGCCTTCACTT |
| *TLR4* | 144 | GCCACATGTCAGGCCTTATG | TTGGTTGAAATGCCCACCTG |
| *MyD88* | 132 | CCCTGGGTGTGTGTGTATCT | CTGCAGACGTGTCTGTGAAG |
| *NF-κB65* | 81 | CCATGGCTGAAGGAAACCAG | AGAGCAAGGAAGTCCCAGAC |
| *TNF-α* | 199 | CGAGTCTGGGCAGGTCTA | GAAGTGGTGGTCTTGTTGC |

**Note:** HMGB1: High mobility group box 1; TLR2: Toll-like receptor 2; TLR4: Toll-like receptor 4; MyD88: Myeloid differentiation primary response gene 88; NF-κB: Nuclear factor kappa B; TNF-α: Tumor necrosis factor-alpha.

30 min, after which they were co-cultured with secondary antibodies. Following a further 30 min of washing with TBST, the membranes were exposed. The bands were photographed and calculated with ImageJ software for plotting purposes (NIH, Bethesda, MD, USA). The experiments were carried out independently and repeated at least three times ($n = 3$).

### *ELISA Experiment to Detect NF-κB Pathway-related Factor Expression*

Following the processing of the cells as outlined above, the respective groups supinates were collected by the instructions stipulated within the ELISA kit ($n = 3$).

### *Statistical Analysis*

Data analysis was conducted using Statistical Package for Social Science (SPSS) software (version 20.0; IBM, Armonk, NY, USA). For comparisons between two groups, unpaired two-sided Student's *t*-tests were applied. Differences among more than two groups were assessed using one-way analysis of variance (ANOVA), followed by Tukey's multiple comparison test where appropriate. A $p$ value less than .05 was considered statistically significant.

## Results

### *CCK8 Assay for Proliferation in Co-cultured THP-1 Macrophages and 16HBE Cells*

Flow cytometry analysis (Figure 1A) demonstrated that THP-1 were efficiently differentiated into macrophages cells following PMA induction, as evidenced by high CD68 expression levels of 98.8%, 99.1%, and 99.3%, respectively. This confirms successful phenotypic transition into macrophages. The CCK8 assay (Figure 1B) revealed that cell proliferation was most robust at a 5:1 ratio of macrophages to 16HBE cells (MC + 16HBE (5:1)), with OD values steadily increasing over time, peaking at 48 and 72 h.

CSE treatment (Figure 1C) significantly inhibited cell proliferation, with stronger effects at higher concentrations. At 4% CSE, OD values significantly decreased, indicating a suppression of cell proliferation. In Figure 1D, when 4% CSE was used as a baseline, adding QBPF (60 and 80 mg/mL) further inhibited cell proliferation, particularly at 24 h, where OD values sharply declined. These results suggest that QBPF (especially at higher concentrations) enhances the suppressive effect of CSE on cell proliferation.

### *Effect of QBPF on Inflammatory Factors*

As illustrated in Figure 2A, stimulation with 4% CSE markedly upregulated several critical inflammatory cytokines, including interleukin (IL)-1β, IL-6, IL-8, NF-κB p65, and tumor necrosis factor-alpha (TNF-α). Conversely, exposure to 20 mg/mL QBPF significantly suppressed the expression of these cytokine markers, suggesting a potent anti-inflammatory effect of QBPF against CSE-triggered responses.

Similarly, qPCR analysis (Figure 2B) revealed a significant upregulation in expression of TLR2, TLR4, myeloid differentiation primary response gene 88 (MyD88), and TNF-α in 16HBE cells following 4% CSE exposure. However, pretreatment with 20 mg/mL QBPF significantly suppressed the expression of these genes, indicating that QBPF inhibit the activation of the NF-κB pathway.

Western blot results (Figure 2C) confirmed these results. After 4% CSE treatment, the expression levels of E-cadherin, HMGB1, MyD88, p65, TLR2, TLR4, and TNF-α were significantly upregulated. However, treatment with 20 mg/mL QBPF reduced the protein expression of these factors, suggesting that the capsules exert an inhibitory effect on the inflammatory response.

As shown in Figure 2D, CSE exposure resulted in pronounced nuclear and cytoplasmic distribution of p65, HMGB1, and TLR4. Notably, QBPF administration led to a considerable attenuation of these protein levels, reinforcing the assumption that the capsules suppress both the production and cellular distribution of CSE-induced pro-inflammatory markers.

### *Effects of 4% CSE on the HMGB1–TLR4–NF-κB Axis*

As illustrated in Figure 3A, ELISA data demonstrated that exposure to 4% CSE markedly elevated the expression of multiple inflammatory mediators, such as IL-1β, IL-6, IL-8, HMGB1, p65, and TNF-α. Silencing NF-κB using siRNA significantly reduced the release of these factors, whereas forced expression via PCDNA3.0 vectors further enhanced their production. Taken together, these findings suggest that NF-κB serves as a key regulatory node in mediating CSE-induced inflammatory signaling and cytokine output.

As shown in Figure 3B, qPCR analysis revealed that 4% CSE exposure led to a significant increase in the transcription of inflammation-related genes, including TLR2, TLR4, MyD88, HMGB1, p65, and TNF-α. Silencing NF-κB markedly suppressed the expression of these targets, whereas its overexpression resulted in a notable enhancement, underscoring the essential regulatory role of NF-κB in CSE-mediated inflammatory gene activation.

Consistently, Western blot analysis (Figure 3C) demonstrated a substantial rise in protein levels of markers such as E-cadherin, HMGB1, MyD88, p65, TLR2, TLR4, and TNF-α following CSE treatment. NF-κB knockdown diminished these protein levels, while forced expression of NF-κB amplified them, confirming its central role in orchestrating CSE-induced inflammatory signaling cascades.

As indicated in Figure 3D, immunofluorescence analysis revealed that 4% CSE exposure markedly increased both the expression and cytoplasmic-to-nuclear translocation of p65,

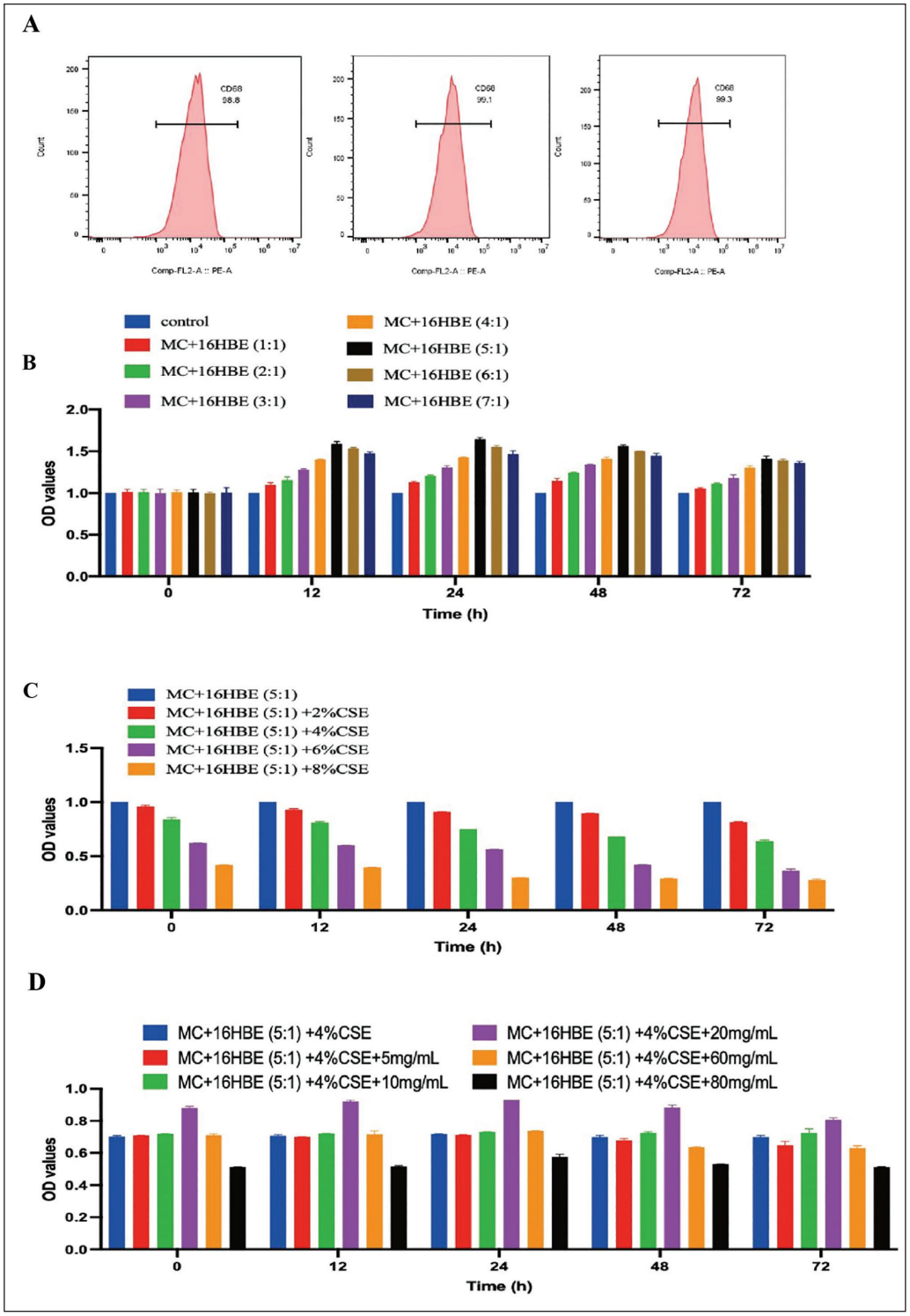



**Figure 1.** Cell Counting Kit-8 (CCK8) Was Used to Detect the Proliferation in Co-culturing THP-1 Macrophages (MC) With 16HBE. (A) Flow Cytometry Analysis of CD68 Expression in Phorbol 12-Myristate 13-Acetate (PMA)-induced THP-1 Cells, Demonstrating Successful Differentiation into MC With CD68 Expression Rates of 98.8%, 99.1%, and 99.3%, Respectively. (B) OD Values Representing Cell Proliferation in Co-culture Systems of THP-1 MC and 16HBE Cells at Various Ratios (1:1, 2:1, 3:1, 4:1, 5:1, 6:1, 7:1) Measured at 0, 12, 24, 48, and 72 h. (C) Effect of Varying Concentrations of Cigarette Smoke Extract (CSE) (2%, 4%, 6%, 8%) on the Proliferation of THP-1 Macrophages and 16HBE Cells Co-cultured at a 5:1 Ratio. (D) Impact of Qibai Pingfei at Different Concentrations (5, 10, 20, 60, 80 mg/mL) Combined With 4% CSE on the Proliferation of Co-cultured HP-1 Macrophages and 16HBE Cells.

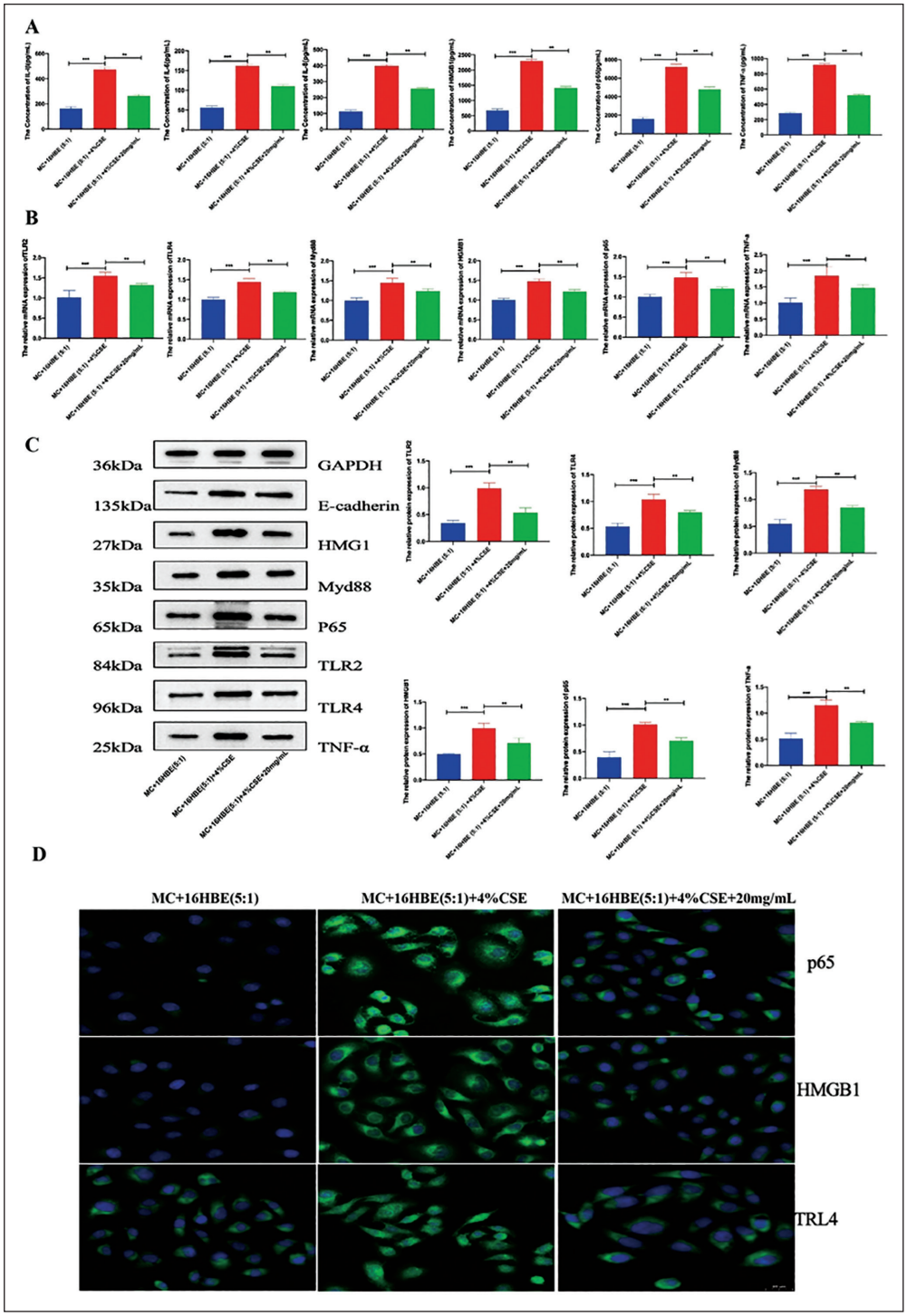



**Figure 2.** The Effect of Qibai Pingfei Capsules on Inflammatory Factors. (A) Enzyme-linked Immunosorbent Assay (ELISA) Analysis of Interleukin (IL)-6, IL-8, IL-1β, Tumor Necrosis Factor-Alpha (TNF-α), and MCP-1 Expression Levels in the Culture Supernatants of THP-1 Macrophages Co-cultured With 16HBE Cells at a 5:1 Ratio, With and Without 4% Cigarette Smoke Extract (CSE) Treatment, and After the Addition of Traditional Medicine (20 mg/mL). (B) Quantitative Reverse Transcription Polymerase Chain Reaction (qRT-PCR) Assessment of the Relative mRNA Expression of Toll-like Receptor 2 (TLR2), Toll-like Receptor 4 (TLR4), Myeloid Differentiation Primary Response Gene 88 (MyD88), p65, and Tumor Necrosis Factor-alpha (TNF-α) Under the Conditions Described in (A). (C) Western Blot Analysis of Protein Expression Levels of TLR2, TLR4, MyD88, p65, and TNF-α, With Glyceraldehyde-3-Phosphate Dehydrogenase (GAPDH) Used as the Loading Control, Following the Same Treatment Conditions as in (A). Bar Graphs Show Protein Quantification Relative to GAPDH. (D) Immunofluorescence Staining Illustrating the Cellular Localization of p65, High Mobility Group Box 1 (HMGB1), and TLR4 in Co-cultured Cells Treated With 4% CSE and Traditional Medicine (80 mg/mL).

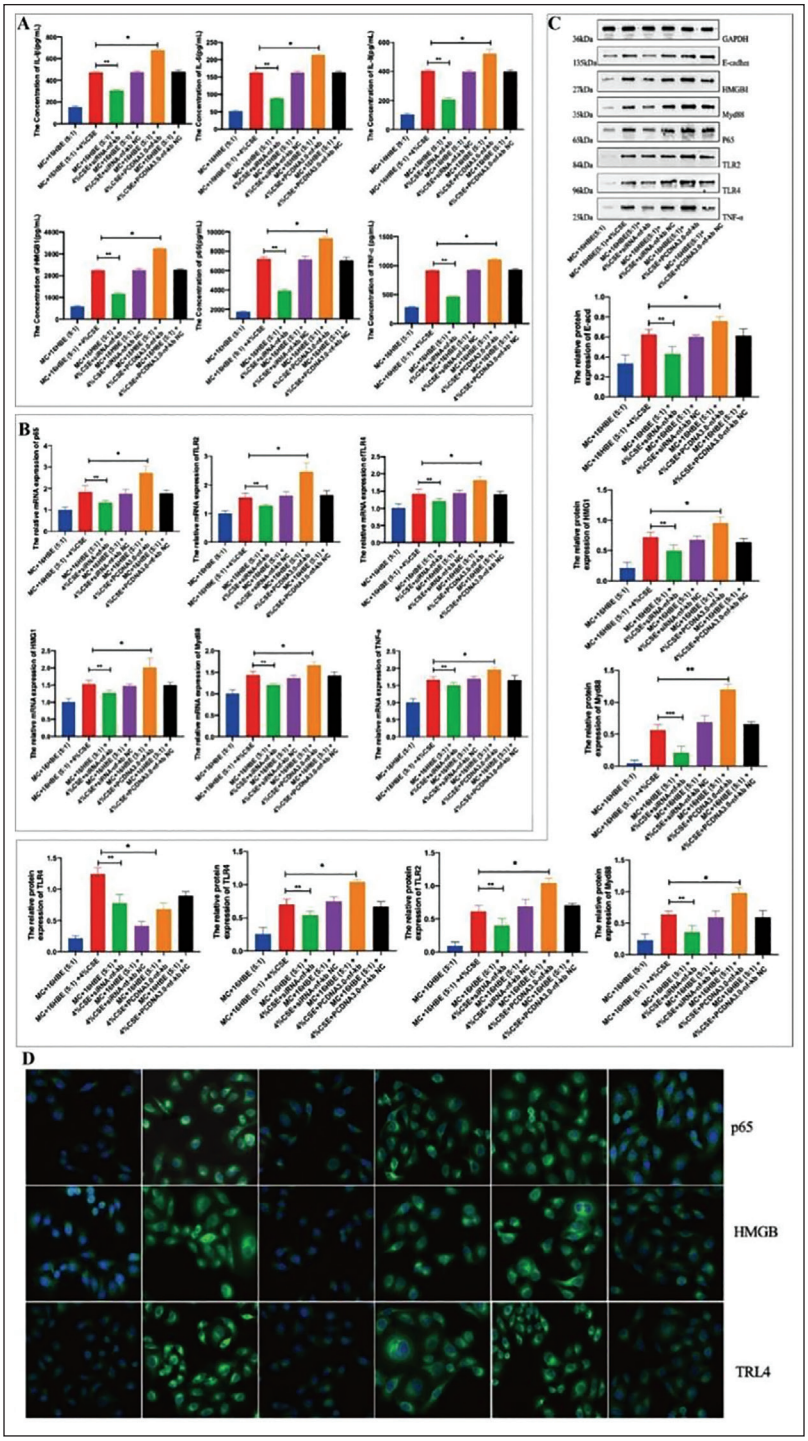



**Figure 3.** The Influence of 4% Cigarette Smoke Extract (CSE) on the High Mobility Group Box 1 (HMGB1)/Toll-like Receptor 4 (TLR4)/Nuclear Factor Kappa B (NF-κB) Signaling Pathway. (A) Enzyme-linked Immunosorbent Assay (ELISA) Results Depicting the Concentrations of Interleukin (IL)-1β, IL-6, IL-8, MCP-1, IL-10, and Tumor Necrosis Factor-Alpha (TNF-α) in the Culture Supernatants of THP-1 Macrophages Co-cultured With 16HBE Cells at a 5:1 Ratio. The Cells Were Treated With 4% Cigarette Smoke Extract (CSE) Alone, 4% CSE+20 mg/mL+siRNA-NF-κB, 4% CSE+20 mg/mL+siRNA-NF-κB NC, 4% CSE+20 mg/mL+PCDNA3.0-NF-κB, or 4% CSE+20 mg/mL+PCDNA3.0-NF-κB NC. (B) Quantitative Reverse Transcription Polymerase Chain Reaction (qRT-PCR) Analysis of the Relative mRNA Expression Levels of TLR2, TLR4, Myeloid Differentiation Primary Response Gene 88 (MyD88), HMGB1, p65, and TNF-α Under the Same Conditions as in (A). (C) Western Blot Analysis of Protein Expression Levels of TLR2, TLR4, MyD88, HMGB1, p65, and TNF-α, With Glyceraldehyde-3-Phosphate Dehydrogenase (GAPDH) as the Loading Control, Under the Same Conditions as in (A). The Bar Graphs Represent the Quantification of Protein Levels Relative to GAPDH. (D) Immunofluorescence Staining Showing the Localization and Expression of p65, HMGB1, and TLR4 Under the Same Conditions as in (A).

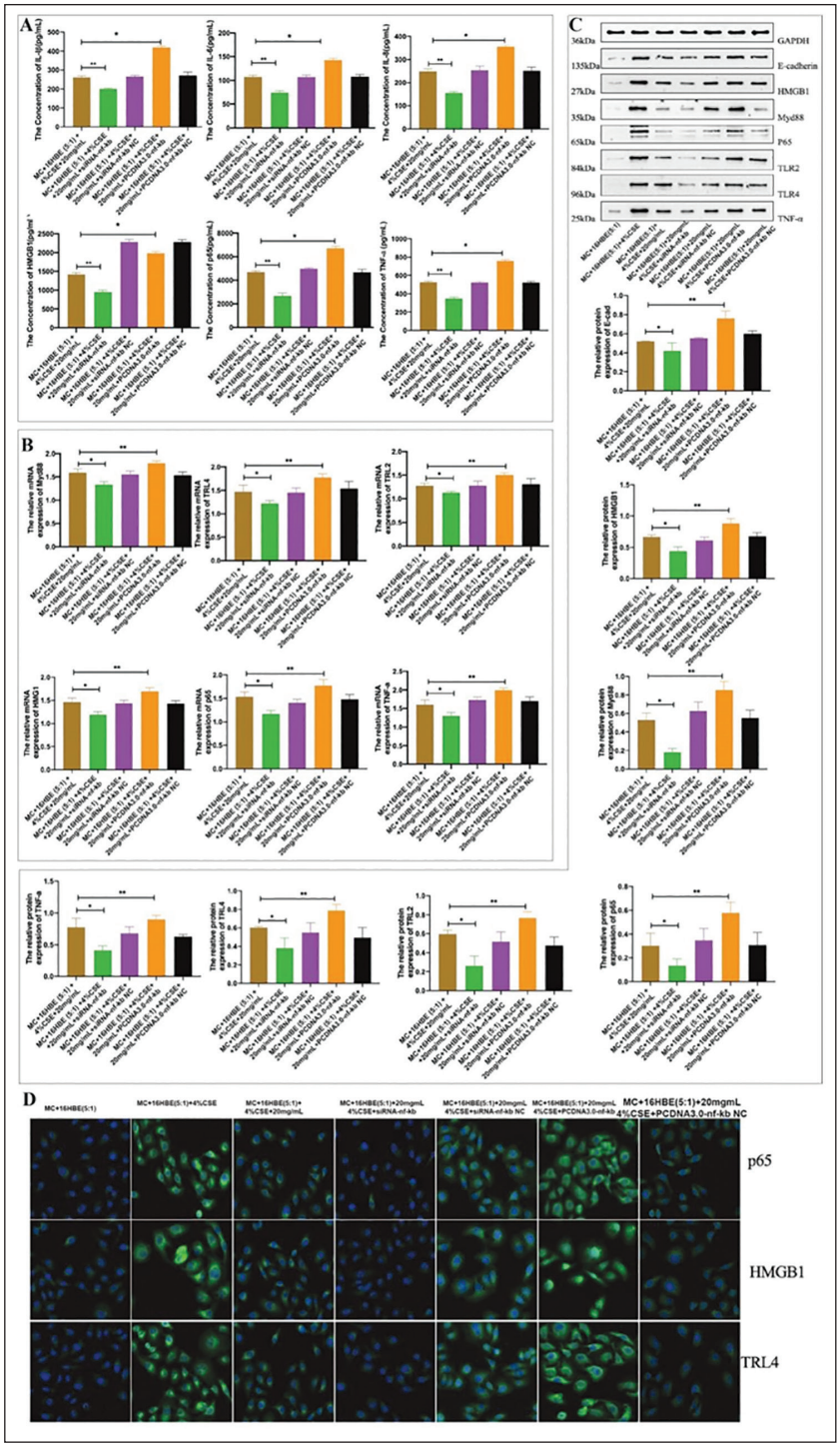



**Figure 4.** The Role of Qibai Pingfei Capsules in Modulating the High Mobility Group Box 1 (HMGB1)/Toll-like Receptor 4 (TLR4)/Nuclear Factor Kappa B (NF-κB) Signaling Pathway. (A) Enzyme-linked Immunosorbent Assay (ELISA) Analysis Showing the Concentrations of Interleukin (IL)-1β, IL-6, IL-8, MCP-1, IL-10, and Tumor Necrosis Factor-Alpha (TNF-α) in the Culture Supernatants of THP-1 Macrophages Co-cultured With 16HBE Cells (5:1 Ratio). Cells Were Treated With 4% Cigarette Smoke Extract (CSE) Alone, Qibai Pingfei 20mg/mL, 4% CSE+20mg/mL+siRNA-NF-κB, 4% CSE+20mg/mL+siRNA-NF-κB NC, 4% CSE+20mg/mL+PCDNA3.0-NF-κB, or 4% CSE+20mg/mL+PCDNA3.0-NF-κB NC. (B) Quantitative Reverse Transcription Polymerase Chain Reaction (qRT-PCR) Analysis of Relative mRNA Expression Levels of Toll-like Receptor 2 (TLR2), TLR4, Myeloid Differentiation Primary Response Gene 88 (MyD88), HMGB1, p65, and TNF-α Under the Same Conditions as in (A). (C) Western Blot Analysis of Protein Expression Levels for TLR2, TLR4, MyD88, HMGB1, p65, and TNF-α, With Glyceraldehyde-3-Phosphate Dehydrogenase (GAPDH) Used as a Loading Control, Under the Same Conditions as in (A). (D) Immunofluorescence Staining of p65, HMGB1, and TLR4 Under the Same Conditions as in (A).

HMGB1, and TLR4. Inhibiting NF-κB activity resulted in diminished levels of these proteins, whereas enhancing its expression produced the reverse outcome, emphasizing NF-κB as a central regulator in CSE-induced inflammatory responses.

### *Role of QBPF in Regulating the HMGB1–TLR4–NF-κB Signaling Pathway*

ELISA analysis (Figure 4A) demonstrated that treatment with 20 mg/mL QBPF deeply declined the protein secretion of IL-1β, IL-6, IL-8, HMGB1, p65, and TNF-α in the supernatant of 16HBE cells. Notably, this effect was even more pronounced following NF-κB knockdown, suggesting that silencing NF-κB can effectively suppress the inflammatory response induced by both CSE and QBPF.

qPCR results (Figure 4B) further confirmed that 20 mg/mL QBPF markedly decreased of inflammation-associated genes such as TLR2, TLR4, MyD88, HMGB1, p65, and TNF-α in 16HBE cells. A more substantial reduction in gene expression has been detected following NF-κB silencing, while NF-κB overexpression resulted in an increased expression of these genes, underscoring the important role of NF-κB in regulating the inflammatory signaling pathway.

Western blot analysis (Figure 4C) corroborated these findings by showing that treatment with 20 mg/mL QBPF significantly reduced the protein expression of E-cadherin, HMGB1, MyD88, p65, TLR2, TLR4, and TNF-α. Silencing NF-κB resulted in a reduction of these protein levels, whereas NF-κB overexpression led to an upregulation of their expression, suggesting that QBPF modulate inflammation through the NF-κB signaling pathway.

Immunofluorescence staining (Figure 4D) showed that exposure to QBPF significantly lowered the content of p65, HMGB1, and TLR4 in 16HBE cells, with the proteins being localized in both the cytoplasm and nucleus. Silencing NF-κB further decreased the expression of these proteins, while NF-κB overexpression increased their levels, further confirming the regulatory function of NF-κB in modulating the inflammation triggered by both CSE and QBPF.

## Discussion

This study explored the anti-inflammatory capacity of QBPF within a CSE-induced 16HBE cell inflammation model, emphasizing the HMGB1-TLR4-NF-κB signaling pathway. Our data showed that 4% CSE significantly elevated the expression of IL-1β, IL-6, IL-8, HMGB1, p65, and TNF-α, contributing to a pronounced pro-inflammatory state. These findings are consistent with previous reports that identified CSE as a potent inducer of inflammation via TLR4-NF-κB pathway activation, which centrally regulates immune responses and host protection (Lee et al., 2021; Ou et al., 2022).

A major insight of this work is the pivotal role of NF-κB as a key inflammation regulator in response to CSE. Silencing NF-κB expression led to a significant decrease in pro-inflammatory cytokines and attenuated the expression of other inflammatory mediators in CSE-stimulated 16HBE cells. This inhibitory action confirms NF-κB's involvement in CSE-induced immune responses, as previously demonstrated (Yang et al., 2016; Zhang et al., 2016). Conversely, NF-κB overexpression further enhanced the inflammatory signaling cascade. Collectively, our findings suggest that NF-κB functions as a central regulatory node in airway inflammation triggered by components of cigarette smoke.

The inflammatory mediators selected in this study (including HMGB1, TLR2, TLR4, MyD88, p65, TNF-α, IL-1β, IL-6, and IL-8) were chosen based on their established involvement in the HMGB1–TLR4–NF-κB pathway, a key driver of CSE-induced airway inflammation. These molecules represent both upstream activators and downstream effectors within the inflammatory cascade. While other factors such as MCP-1, IL-17, and IFN-γ also contribute to smoke-related immune responses, the current investigation focused specifically on targets regulated by NF-κB, aiming to better elucidate the therapeutic mechanisms of QBPF within this canonical signaling context.

A key observation from this study is that QBPF significantly alleviated CSE-evoked inflammatory responses. This was evidenced by a marked decrease in the release of typical pro-inflammatory mediators (e.g., IL-1β, IL-6, IL-8, TNF-α) and reduced expression of inflammation-related regulatory targets—including TLR2, TLR4, MyD88, HMGB1, and p65—at both the transcriptional and translational levels. These findings indicate that QBPF exhibits a multi-level anti-inflammatory effect, likely by interfering with the TLR4/NF-κB axis. Moreover, immunofluorescence imaging revealed that QBPF treatment impaired NF-κB nuclear translocation, a prerequisite for its pro-inflammatory gene activation, underscoring the compound's role in disrupting key checkpoints in inflammation signaling.

Considering the persistent airway inflammation commonly associated with smoking-related diseases such as COPD, our results imply that QBPF has the potential to disrupt key upstream and downstream mediators involved in the HMGB1/TLR4/NF-κB axis. This modulatory effect may contribute to delaying disease progression and attenuating tissue damage. *In vitro* findings underscore the therapeutic potential of QBPF in controlling chronic inflammation. Nevertheless, further research is essential to assess its clinical efficacy and confirm its suitability as an anti-inflammatory strategy for smoke-induced pulmonary diseases.

Despite the exciting results of the present study, there are still some restrictions that deserve to be noted in future studies. Firstly, while our *in vitro* results demonstrate the anti-inflammatory function of QBPF in CSE-induced inflammation in 16HBE cells, the findings are based on a single cell line and may not fully reflect the complexity of the *in vivo*

environment. To further elucidate the therapeutic value of QBPF, subsequent investigations in appropriate animal models are warranted to assess its physiological relevance and potential systemic impact. While the current study highlights the modulation of the HMGB1–TLR4–NF-κB axis, additional work should aim to uncover alternative signaling routes involved in its anti-inflammatory effects. Future studies should also define key pharmacological parameters—including dosage range, treatment course, and safety thresholds—under clinically relevant conditions. Given the prolonged nature of airway inflammation and associated tissue remodeling, long-term evaluations will be essential. Addressing these knowledge gaps will contribute to a more comprehensive understanding of QBPF's mode of action and support its translation into targeted therapies for chronic smoke-related disorders.

## Conclusion

In summary, this study highlights the therapeutic promise of QBPF in counteracting CSE-induced airway inflammation, likely through interference with key inflammatory cascades including the HMGB1–TLR4–NF-κB axis. While the *in vitro* data offer encouraging insights, further studies involving animal models are necessary to evaluate the compound's pharmacodynamic profile, systemic tolerance, and long-term biological effects. In addition, the clinical applicability of QBPF requires rigorous assessment regarding appropriate dosing strategies, treatment duration, and translational relevance in human disease contexts. For conditions characterized by persistent inflammation, such as COPD, future investigations should determine whether extended administration of QBPF can confer sustained benefits and positively influence disease progression. Taken together, these findings provide a rationale for advancing QBPF into further preclinical and clinical research pipelines as a candidate intervention for smoking-related and chronic inflammatory disorders.

### Abbreviations

ANOVA: Analysis of variance; CCK8: Cell Counting Kit-8; CSE: Cigarette smoke extract; DAMP: Damage-associated molecular pattern; ELISA: Enzyme-linked immunosorbent assay; HMGB1: High mobility group box 1; MyD88: Myeloid differentiation primary response gene 88; PMA: Phorbol 12-myristate 13-acetate; QBPF: Qibai Pingfei Capsules; qRT-PCR: Quantitative reverse transcription polymerase chain reaction; RPMI-1640: Roswell Park Memorial Institute-1640; SPSS: Statistical Package for Social Science; TCM: Traditional Chinese medicine; TLR2: Toll-like receptor 2.

### Declaration of Conflicting Interests

The authors declared no potential conflicts of interest with respect to the research, authorship, and/or publication of this article.

### Ethical Approval and Informed Consent

NA.

### Funding

The authors disclosed receipt of the following financial support for the research, authorship, and/or publication of this article: This work was supported by the National Natural Science Foundation of China (No. 82104780).

### ORCID iD

Zegeng Li https://orcid.org/0009-0007-8881-1682

### References

Chen, R., Kang, R., & Tang, D. (2022). The mechanism of HMGB1 secretion and release. *Experimental and Molecular Medicine*, *54*(2), 91–102. https://doi.org/10.1038/s12276-022-00736-w

Christenson, S. A., Smith, B. M., Bafadhel, M., & Putcha, N. (2022). Chronic obstructive pulmonary disease. *The Lancet*, *399*(10342), 2227–2242. https://doi.org/10.1016/S0140-6736(22)00470-6

Elisia, I., Lam, V., Cho, B., Hay, M., Li, M. Y., Yeung, M., Bu, L., Jia, W., Norton, N., Lam, S., & Krystal, G. (2020). The effect of smoking on chronic inflammation, immune function and blood cell composition. *Scientific Reports*, *10*(1), Article 19480. https://doi.org/10.1038/s41598-020-76556-7

Facchinetti, F., Amadei, F., Geppetti, P., Tarantini, F., Di Serio, C., Dragotto, A., Gigli, P. M., Catinella, S., Civelli, M., & Patacchini, R. (2007). Alpha,beta-unsaturated aldehydes in cigarette smoke release inflammatory mediators from human macrophages. *American Journal of Respiratory Cell and Molecular Biology*, *37*(5), 617–623. https://doi.org/10.1165/rcmb.2007-0130OC

Idoudi, S., Bedhiafi, T., Pedersen, S., Elahtem, M., Alremawi, I., Akhtar, S., Dermime, S., Merhi, M., & Uddin, S. (2023). Role of HMGB1 and its associated signaling pathways in human malignancies. *Cellular Signalling*, *112*, Article 110904. https://doi.org/10.1016/j.cellsig.2023.110904

Jia, Y., He, T., Wu, D., Tong, J., Zhu, J., Li, Z., & Dong, J. (2022). The treatment of Qibai Pingfei Capsule on chronic obstructive pulmonary disease may be mediated by Th17/Treg balance and gut-lung axis microbiota. *Journal of Translational Medicine*, *20*(1), 281. https://doi.org/10.1186/s12967-022-03481-w

Kosmider, B., Messier, E. M., Chu, H. W., & Mason, R. J. (2011). Human alveolar epithelial cell injury induced by cigarette smoke. *PLoS One*, *6*(12), Article e26059. https://doi.org/10.1371/journal.pone.0026059

Kotlyarov, S. (2023). The role of smoking in the mechanisms of development of chronic obstructive pulmonary disease and atherosclerosis. *International Journal of Molecular Sciences*, *24*(10), Article 8725. https://doi.org/10.3390/ijms24108725

Le, Y., Wang, Y., Zhou, L., Xiong, J., Tian, J., Yang, X., Gai, X., & Sun, Y. (2020). Cigarette smoke-induced HMGB1 translocation and release contribute to migration and NF-kappaB activation through inducing autophagy in lung macrophages. *Journal of Cellular and Molecular Medicine*, *24*(2), 1319–1331. https://doi.org/10.1111/jcmm.14789

Lee, K.-H., Woo, J., Kim, J. Y., Lee, C.-H., & Yoo, C.-G. (2021). Cigarette smoke extract-induced downregulation of p300 is responsible for the impaired inflammatory cytokine response of macrophages. *Cellular Signalling*, *85*, Article 110050. https://doi.org/10.1016/j.cellsig.2021.110050

Leiter, A., Veluswamy, R. R., & Wisnivesky, J. P. (2023). The global burden of lung cancer: Current status and future trends. *Nature Reviews. Clinical Oncology*, *20*(9), 624–639. https://doi.org/10.1038/s41571-023-00798-3

Liu, T., Zhang, L., Joo, D., & Sun, S.-C. (2017). NF-kappaB signaling in inflammation. *Signal Transduction and Targeted Therapy*, *2*, Article 17023. https://doi.org/10.1038/sigtrans.2017.23

Ou, G., Zhu, M., Huang, Y., Luo, W., Zhao, J., Zhang, W., Xia, H., Wang, S., He, R., Xiao, Q., Deng, Y., & Qiu, R. (2022). HSP60 regulates the cigarette smoke-induced activation of TLR4-NF-kappaB-MyD88 signalling pathway and NLRP3 inflammasome. *International Immunopharmacology*, *103*, Article 108445. https://doi.org/10.1016/j.intimp.2021.108445

Wang, M., Gauthier, A., Daley, L., Dial, K., Wu, J., Woo, J., Lin, M., Ashby, C., & Mantell, L. L. (2019). The role of HMGB1, a nuclear damage-associated molecular pattern molecule, in the pathogenesis of lung diseases. *Antioxidants and Redox Signaling*, *31*(13), 954–993. https://doi.org/10.1089/ars.2019.7818

Wang, C., Zhou, J., Wang, J., Li, S., Fukunaga, A., Yodoi, J., & Tian, H. (2020). Progress in the mechanism and targeted drug therapy for COPD. *Signal Transduction and Targeted Therapy*, *5*(1), 248. https://doi.org/10.1038/s41392-020-00345-x

Yang, J., Yu, H. M., Zhou, X. D., Huang, H. P., Han, Zh., Kolosov, V. P., & Perelman, J. M. (2016). Cigarette smoke induces mucin hypersecretion and inflammatory response through the p66shc adaptor protein-mediated mechanism in human bronchial epithelial cells. *Molecular Immunology*, *69*, 86–98. https://doi.org/10.1016/j.molimm.2015.11.002

Ying, Y., Sun, C. B., Zhang, S. Q., Chen, B. J., Yu, J. Z., Liu, F. Y., Wen, J., Hou, J., Han, S. S., Yan, J. Y., Yang, Z. S., & Xiong, L. (2021). Induction of autophagy via the TLR4/NF-kappaB signaling pathway by astragaloside IV contributes to the amelioration of inflammation in RAW264.7 cells. *Biomedicine and Pharmacotherapy*, *137*, Article 111271. https://doi.org/10.1016/j.biopha.2021.111271

Yoshida, M., Minagawa, S., Araya, J., Sakamoto, T., Hara, H., Tsubouchi, K., Hosaka, Y., Ichikawa, A., Saito, N., Kadota, T., Sato, N., Kurita, Y., Kobayashi, K., Ito, S., Utsumi, H., Wakui, H., Numata, T., Kaneko, Y., Mori, S. & Kuwano, K. (2019). Involvement of cigarette smoke-induced epithelial cell ferroptosis in COPD pathogenesis. *Nature Communications*, *10*(1), 3145. https://doi.org/10.1038/s41467-019-10991-7

Yu, H., Lin, L., Zhang, Z., Zhang, H., & Hu, H. (2020). Targeting NF-kappaB pathway for the therapy of diseases: Mechanism and clinical study. *Signal Transduction and Targeted Therapy*, *5*(1), 209. https://doi.org/10.1038/s41392-020-00312-6

Zhang, C., Qin, S., Qin, L., Liu, L., Sun, W., Li, X., Li, N., Wu, R., & Wang, X. (2016). Cigarette smoke extract-induced p120-mediated NF-kappaB activation in human epithelial cells is dependent on the RhoA/ROCK pathway. *Scientific Reports*, *6*, Article 23131. https://doi.org/10.1038/srep23131

Zhu, J., Wang, B., Lu, M., Tong, J., Yang, C., & Li, Z. (2018). Effects of Qibaipingfei capsules on pulmonary vascular relaxation through KATP channel activation by the NO/cGMP signaling pathway. *Pakistan Journal of Pharmaceutical Sciences*, *31*(2), 545–552.